

Study on Evaluation of Seismic Pounding Behavior of Adjacent Traditional Wooden Houses

M. Sugino, N. Takiyama, Y. Onishi & Y. Hayashi

Kyoto University, Japan

H. Takahashi

Shimizu Corporation, Japan



SUMMARY:

There are a lot of traditional wooden houses all over Japan and some of them stand closely each other. Thus, pounding can occur between two houses under a strong ground motion. The objective of this study is to establish a method of evaluating whether a pounding arises or not between adjacent traditional wooden houses especially by pulse-like strong ground motions arisen from inland earthquakes. To evaluate the interval between two houses, the SPD (spectral difference) rule is effective in random vibration. When shaken by a pulse wave, the interval can be evaluated from the relation between the pulse period and the natural periods of two houses. And if pounding occurs, their behavior can be simulated by nonlinear time history response analysis.

Keywords: Traditional wooden houses, Shaking table test, Simulation analysis, Pulse-like ground motions

1. INTRODUCTION

In Japan, there are a lot of traditional wooden houses which suit for the climate and the natural features in every district. Some of wooden houses stand closely each other like in *Narai* and in *Ineura* (Fig.1.1). Thus, pounding can occur between two houses under strong ground motion. Hayashi et al. (2009) performed microtremor measurements of groups of traditional wooden houses to confirm these houses standing by themselves or contacting with each other. But little attention has been given to seismic pounding behavior of adjacent traditional wooden houses. To confirm the safety of the traditional wooden houses, it is not enough just to evaluate the aseismic performance of each house, but it is necessary to consider the influence of adjacent houses.



(a) *Narai*, Nagano



(b) *Ineura*, Kyoto

Figure 1.1. Traditional wooden houses standing closely

In Kyoto, traditional houses called “*Kyomachiya*” stand very closely with each other. Kyoto is less affected from subduction zone earthquake such like Nankai and Tonankai earthquake because Kyoto is away from hypocentral region of these earthquakes. However, inland earthquakes may occur to no small extent. Therefore, it is more important to confirm the influence by inland earthquake than by subduction zone earthquake. Pulse-like strong ground motions arise from inland earthquakes such like the Hyogo-ken Nambu earthquake in 1995. These ground motions have destructive power even if their wave number is few. For this reason, it is important to grasp the behavior of traditional wooden houses shaken by pulse-like strong ground motions.

The objective of this study is to establish a method estimating whether a pounding arises or not between adjacent traditional wooden houses and evaluating seismic pounding behavior when

pounding occurs especially by pulse-like strong ground motions of inland earthquake. The shaking table test of wooden frame structure is conducted to compare the behavior of adjacent wooden houses evaluated from the method proposed in this study with the behavior of specimens in the experiment. In the experiment, both non-pounding experiment and pounding experiment are performed.

2. POUNDING EXPERIMENT OF WOODEN FRAME STRUCTURE

2.1. Experimental method

2.1.1 Specimens

Six types of wooden frame structures and one steel frame structure shown in Fig. 2.1 are used in this experiment. Simple wooden frame called SF in this paper is composed of column, foundation and beam. BF is wooden frame structure added large section beam called *Sashigamoi* to SF. HF is wooden frame structure added hanging wall made of dry mud panel called *Arakabe panel* on one side of SF. BHF has both large section beam and hanging wall on both sides. WW is wooden frame and entire wall structure which is composed of weatherboarding called *Shitamita*. EW is wooden frame and entire wall structure which is composed of dry mud panel on one side. S has H-shaped steel beam.

Specimens are composed of two parallel wooden structures and top board (plywood and binding beam) and stainless steel brace. There is a weight on the top board. We refer to the past loading experiments [Yamada et al. (2004) and Morii et al. (2010)], and determine the weight not to float the base of column. Specimens are fixed to the foundation on the shaking table with the anchor bolt. Table 2.1 shows the details of the specimens. f_0 is the natural frequency before excitation. Columns of all specimens are made of Japanese cedar (E70 in Japanese Agricultural Standard). *Sashigamoi* of BF and BHF is made of Oregon pine E110 and its cross section is 120x270mm. Column - beam or foundation joint of SF, HF, WW and EW are mortise joint (30x84x52.5cm) and held with the metal plate from both side. In case of BF and BHF, joint is mortise joint (capital: 30x80x150cm, base of column: 30x80x100cm) with 15x15cm Oregon pine pin. Thickness of dry mud panel is 26mm.

Table 2.1. Details of specimens

Case	1		2		3		4	
Specimen	SF	WW	SF	EW	BF	BHF	HF	S
Width (mm)	1820	1820	1820	1820	1820	1820	1820	1820
Height of column (mm)	2625	2625	2625	2625	2610	2610	2625	2625
Column cross section (mm)	105x105	105x105	105x105	105x105	120x120	120x120	105x105	H-125x125x6.5x9
Loading weigh (kN)	22.0	22.6	22.0	32.8	32.5	23.4	22.6	23.5
f_0 (Hz)	0.9	5.6	0.9	4.8	1.4	1.8	1.5	4.1

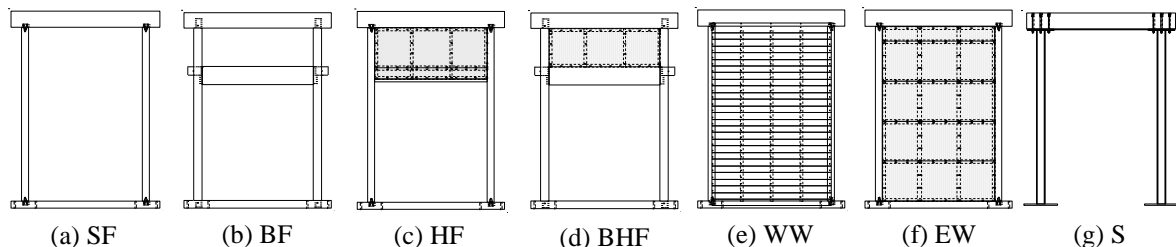


Figure 2.1. Elevations of specimens

2.1.2 Input Waves

Shaking table is excited in one direction, and displacement control is carried out. Sinusoidal pulse, ricker wavelet and the random wave are used in this experiment. Table 2.2 shows the excitation schedule.

The acceleration of the sinusoidal pulse is made by one cycle of sine wave. The displacement

waveform is shown in Fig. 2.2 (a). There are four types of sinusoidal pulse that their periods T_p are 0.5, 1.0, 2.0, and 3.0s. And their maximum displacement D_0 is 250mm except for $T_p = 0.5$ s. Under the condition $T_p = 0.5$ s, we decrease D_0 to 200mm because of the response of specimens becoming too excessive. The period of ricker wavelet is fixed to $T_p = 0.7$ s and their amplitude gains gradually until specimens collide mutually. The displacement waveform is shown in Fig. 2.2 (b). Sinusoidal pulse and ricker wavelet are called pulse wave in this experiment.

In contrast, random wave which continues long time is also used in this experiment to compare to sinusoidal pulse. Random wave is simulated ground motion which continues for 165s and made by using the random phase and the standard acceleration response spectra (damping ratio 5%) on free engineering bedrock compliant with the safety limit (level 2) in the building standard law of Japan. In this study, four waves which change amplitude are input. Figure 2.2 (c) shows displacement waveform.

Sinusoidal pulse No.4 ($T_p = 1.0$ s) , random wave (No.12) and ricker wavelet (No.13~14) are executed the pounding experiment setting on load cell to evaluate pounding behavior.

Table 2.2. Schedule of input wave

No.	Input wave	T_p (s)	D_0 (mm)	Amp. (%)	Pounding
1	Sinusoidal pulse	3.0	250	-	-
2		2.0			
3		1.0			
4		1.0			
5		0.5	200		-
6		0.5			
7		1.0	250		-
8		2.0			
9	Random wave	-	36	20	-
10			90	50	
11			125	70	
12			179	100	
13	Ricker wavelet	0.7	100	40	O
14			150	60	
15			200	80	
16			250	100	

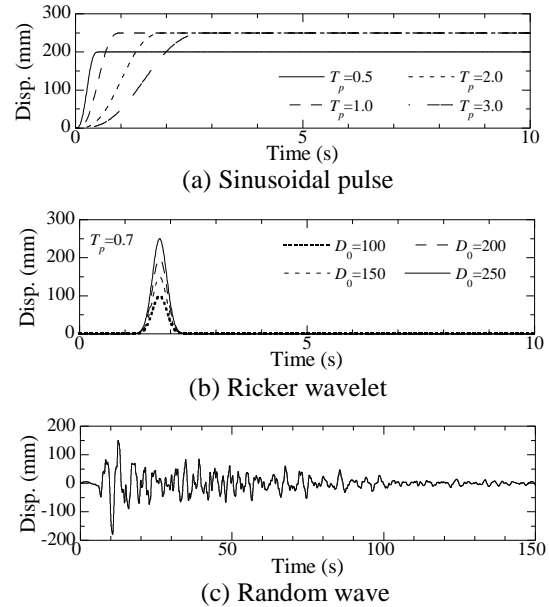


Figure 2.2. Input waves

2.1.3 Measurement method

Figure 2.3 shows the position of measuring instrument of specimens. To confirm pounding behavior, accelerometers and displacement meters are set up on the top and bottom of specimens. Each analysis data is the average of two measurement data. Load cells are also equipped on the top of each specimen to confirm pounding load between specimens. They are removable and equipped only for pounding experiment. Distance between two buildings (specimens) before excitation is named “Clearance” in this paper. Distance between two buildings during excitation is named ‘Interval’ and subtraction of displacement of each building is named “Relative displacement” respectively. Interval and relative displacement change during excitation. Clearance changes depending on residual deformation by past excitation. There is a relation between three values shown below.

$$(\text{Interval}) = (\text{Clearance}) - (\text{Relative displacement})$$

Pounding occurs when relative displacement exceeds clearance. Clearance setting a load cell on specimen is about 125mm, and when removing a load cell it is about 250mm.

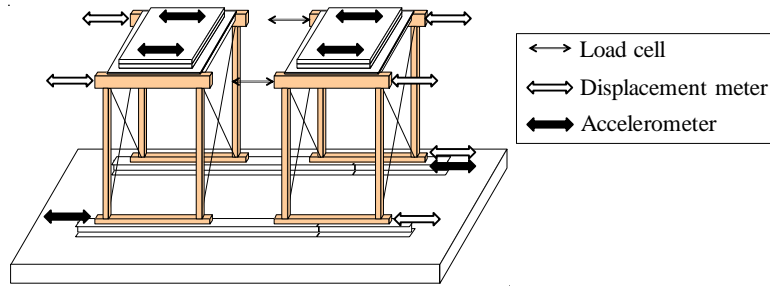


Figure 2.3. The position of measuring instruments

2.2. Experimental conclusion

Figure 2.4 shows the typical response acceleration and displacement of specimens in pounding experiment. They are time history wave of SF and WW excited by $T_p = 1.0s$. When pounding occurs, acceleration increases rapidly while displacement changes gradually. Figure 2.5 indicates pounding load excited by sinusoidal pulse or random wave. The number of pounding times is only one or two times in pulse wave although there are many pounding times in random wave.

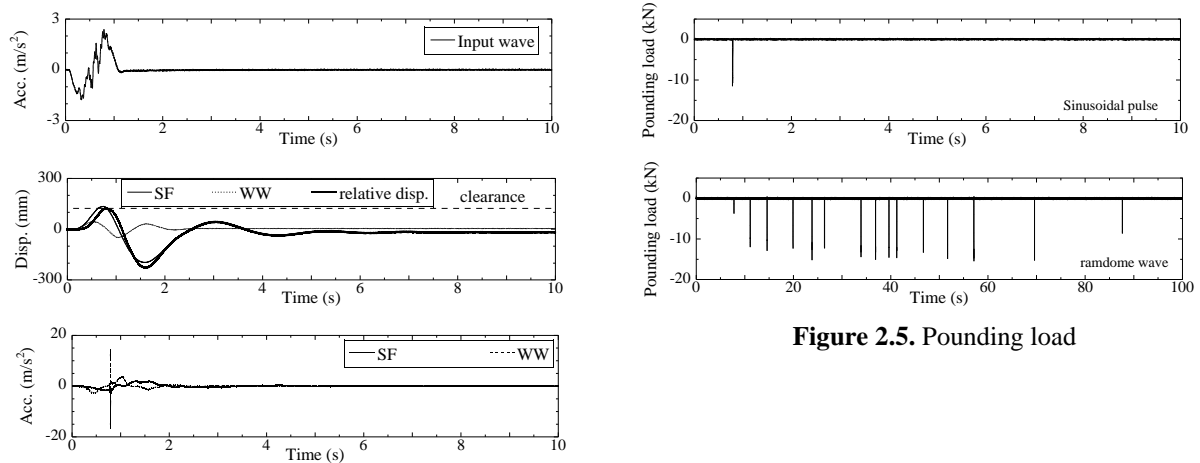


Figure 2.5. Pounding load

Figure 2.4. Pounding experiment
(Case1 sinusoidal pulse No.4)

3. EVALUATION OF POUNDING BEHAVIOR OF ADJACENT WOODEN HOUSES

3.1. Flow chart of pounding behavior evaluation

Evaluation of pounding behavior consists of two parts; probability of pounding and behavior during pounding. The flow chart shows in Fig. 3.1. Δ_1 and Δ_2 are displacement of each building (specimen). $(\Delta_1 - \Delta_2)$ is relative displacement. In evaluating probability of pounding, maximum displacement of each building $|\Delta_i|_{\max}$ ($i=1, 2$) without pounding is calculated from response spectrum method. Maximum relative displacement $|\Delta_1 - \Delta_2|_{\max}$ is evaluated from the SPD (spectral difference) rule [Kasai et al. (2009)].

If $|\Delta_1 - \Delta_2|_{\max}$ is larger than clearance, two buildings collide with each other. Then, non-linear time history analysis with pounding is executed to evaluate behavior during pounding.

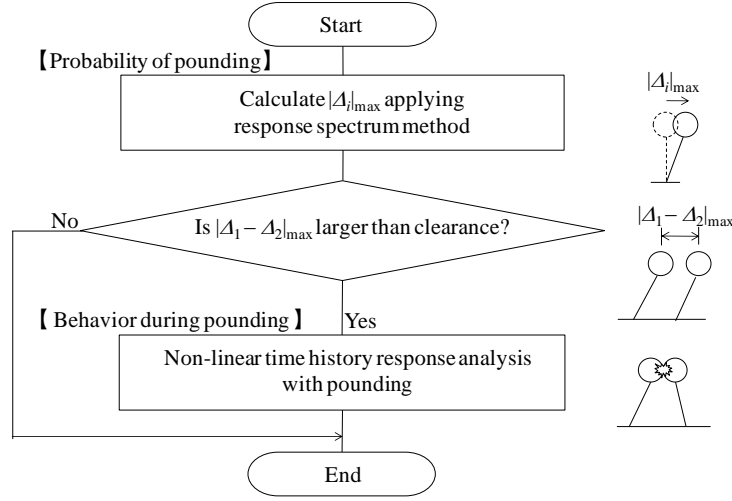


Figure 3.1. Flow chart of pounding evaluation behavior

3.2. Maximum response evaluation using response spectrum method

Maximum displacement of each building $|\Delta_i|_{\max}$ ($i=1, 2$) without pounding is calculated from response spectrum method. As Eqs. (3.1) ~ (3.4) indicate, this method transforms the skeleton curve of buildings into the equivalent response spectra S_{ae} of the same damping ratio.

$$T_e = 2\pi \sqrt{\frac{RH_e}{(M/M_e)C_y g}} \quad (3.1)$$

Where T_e = the equivalent period of the buildings, R = deformation angle, H_e = effective height, M = total mass, M_e = effective mass, C_y = yield base shear coefficient, g = gravitational acceleration.

$$h_e = 0.2(1 - 1/\max(\sqrt{R/R_y}, 1)) + 0.05 \quad (3.2)$$

Where h_e = the equivalent damping ratio, R_y = yield deformation angle.

$$F_h = (1 + 0.05\alpha)/(1 + h_e\alpha) \quad (3.3)$$

Where F_h = reduction factor, α = coefficient of input wave; when input wave is sinusoidal pulse, $\alpha = \pi$, input wave is random wave, $\alpha = 10$.

$$S_{ae} = (2\pi/T_e)^2 RH_e / F_h \quad (3.4)$$

Where S_{ae} = the equivalent response spectra of the buildings. S_{ae} is directly comparable to the response spectra S_a of ground motions. The point of intersection showed in Fig. 3.2 is the maximum response. In this study, skeleton curve is represented by perfect elasto - plasticity fitting to the experiment without pounding like Fig. 3.3. Table 3.1 indicates the parameter of skeleton curve.

Figure 3.4 shows maximum displacement $|\Delta_i|_{\max}$ divided by maximum ground motion D_0 ; D_0 is an experimental value or a result of response spectrum method. Response spectrum method estimates well in large displacement although it estimates smaller than experiment in small displacement. This is because stiffness of the model is too large in small displacement. It is a future research issue to make skeleton curve high precision.

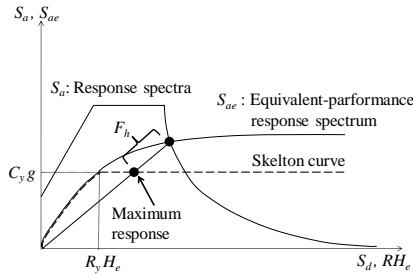


Figure 3.2. Response spectrum method

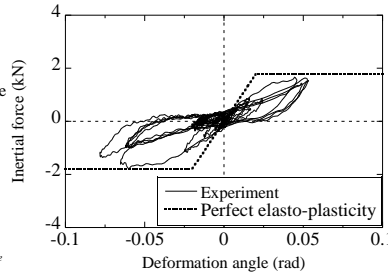


Figure 3.3. The model of perfect elasto-plasticity

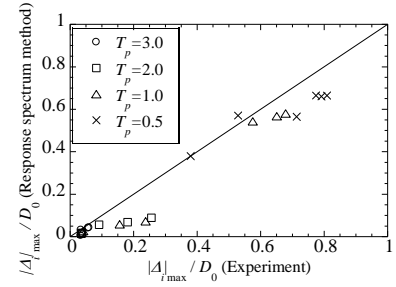


Figure 3.4. Maximum displacement calculated by response spectrum method and experiment

Table 3.1. Parameter of skeleton curve

CASE	1		2		3		4	
Specimens	SF	WW	SF	EW	BF	BHF	HF	S
C_y	0.18	0.44	0.16	1.12	0.21	0.72	0.44	1.82
R_y (rad)	0.02	0.01	0.02	0.01	0.02	0.02	0.02	—
H_e (mm)	2625	2625	2625	2625	2610	2610	2625	2620
M/M_e	1.00	1.00	1.00	1.00	1.00	1.00	1.00	1.00

3.3. Evaluation of probability of pounding

Probability of pounding is judged whether maximum relative displacement $|\Delta_1 - \Delta_2|_{\max}$ is larger than clearance or not. $|\Delta_1 - \Delta_2|_{\max}$ is evaluated from the SPD rule Eqs. (3.5) and (3.6) below.

$$|\Delta_1 - \Delta_2|_{\max} = \sqrt{|\Delta_1|_{\max}^2 + |\Delta_2|_{\max}^2 - 2\rho_{12}|\Delta_1|_{\max}|\Delta_2|_{\max}} \quad (3.5)$$

$$\rho_{12} = \frac{8\sqrt{h_{e1}h_{e2}}(h_{e2} + \beta^*h_{e1})\beta^{*1.5}}{(1 - \beta^{*2})^2 + 4h_{e1}h_{e2}(1 + \beta^{*2})\beta^* + 4(h_{e1} + h_{e2})\beta^{*2}} \quad (3.6)$$

Where ρ_{12} = a cross correlation coefficient, β^* = ratio of effective vibration T_{e2}/T_{e1} , h_{ei} = effective damping ratios.

First, Fig. 3.5 shows the estimated maximum relative displacement $|\Delta_1 - \Delta_2|_{\max}$ applying maximum response $|\Delta_i|_{\max}$ calculated by response spectrum method using perfect elasto-plasticity model to the SPD rule and experimental $|\Delta_1 - \Delta_2|_{\max}$. The estimated $|\Delta_1 - \Delta_2|_{\max}$ is smaller than experimental $|\Delta_1 - \Delta_2|_{\max}$ because estimated $|\Delta_i|_{\max}$ by response spectrum method estimates smaller than the experimental value. Thus in Fig. 3.6, estimated $|\Delta_1 - \Delta_2|_{\max}$ is calculated to apply experimental $|\Delta_i|_{\max}$ to the SPD rule. T_{ei} is evaluated from the peak of a fourier spectrum ratio divided the measured value on the specimen by the measured value under the specimen measured by accelerometer during excitation. h_{ei} is calculated by energy balance Eq. (3.7) below.

$$h_{ei} = \frac{-\int_0^T \ddot{x} \dot{y} dt}{2 \cdot (2\pi / T_{ei}) \cdot \int_0^T \dot{y}^2 dt} \quad (3.7)$$

Where \ddot{x} = acceleration on the ground, \dot{y} = relative velocity, T = measurement time.

In Fig. 3.6 (b), the SPD rule is able to evaluate the maximum relative displacement $|\Delta_1 - \Delta_2|_{\max}$ in random wave. In pulse wave, $|\Delta_1 - \Delta_2|_{\max}$ is categorized into three types according to the relation between T_{e1} and T_p in Fig. 3.6 (a). Figure 3.6 (a) indicates that the SPD rule evaluate with low precision when T_p is longer than T_{e1} . Thus, we suggest the expression of inequality to grasp $|\Delta_1 - \Delta_2|_{\max}$ approximately in Eq. 3.8 below.

$$\begin{aligned} T_{e2} < T_{e1} < T_p, \quad & |\Delta_1 - \Delta_2|_{\max} \leq 0.4D_0 \\ T_{e2} < T_p \leq T_{e1}, \quad & 0.4D_0 \leq |\Delta_1 - \Delta_2|_{\max} \leq 1.4D_0 \\ T_p \leq T_{e2} \leq T_{e1}, \quad & |\Delta_1 - \Delta_2|_{\max} \leq 2.0D_0 \end{aligned} \quad (3.8)$$

Where D_0 = maximum ground motion. This tendency is described by Fig. 3.7 and Fig. 3.8. When $T_{e2} < T_{e1} < T_p$, the probability of pounding is low because the maximum displacement $|\Delta_i|_{\max}$ is small in both buildings. When $T_{e2} < T_p \leq T_{e1}$, $|\Delta_1|_{\max}$ becomes large nearly to D_0 because T_{e1} is larger than T_p and $|\Delta_1 - \Delta_2|_{\max}$ also becomes large. Thus the probability of pounding becomes high. When $T_p \leq T_{e2} \leq T_{e1}$, $|\Delta_i|_{\max}$ of both buildings are large but the probability of pounding is low because they vibrate at nearly coordinate phase during excitation. But in free vibration after excitation, their phases shift according to each T_{ei} and when their phases become opposite, the probability of pounding becomes high.

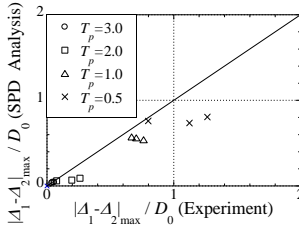


Figure 3.5. Experimental displacement vs. Estimated displacement

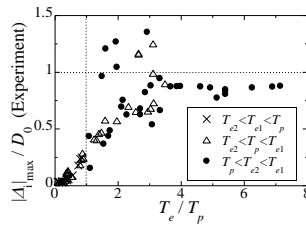
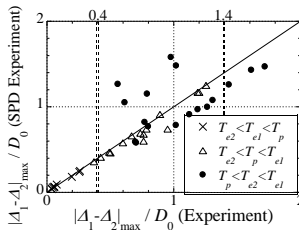
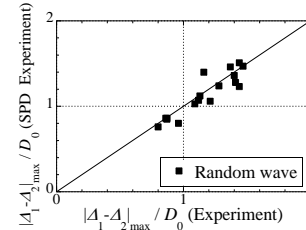


Figure 3.7. Relation between $|\Delta_i|_{\max}$ and T_{ei}

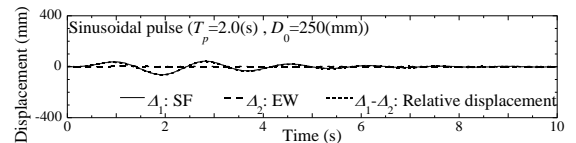


(a) Pulse wave

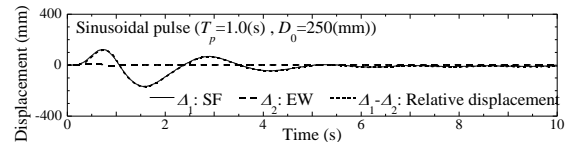


(b) Random wave

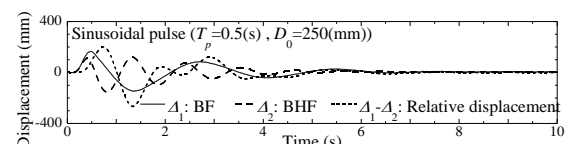
Figure 3.6. Experimental displacement vs. Estimated displacement



(a) $T_{e2} < T_{e1} < T_p$



(b) $T_{e2} < T_p \leq T_{e1}$



(c) $T_p \leq T_{e2} \leq T_{e1}$

Figure 3.8. Experimental displacement vs. Estimated displacement

3.4. Establishment of pounding model for simulation analysis

3.4.1. Non-linear time history response analysis with pounding

Figure 3.9 shows the SDOF models are put side by side with clearance. A pounding linear spring between buildings works when relative displacement ($\Delta_1 - \Delta_2$) exceeds clearance. External force P is represented the equation below.

$$P = K_p (\Delta_1 - \Delta_2) + c_p (\dot{\Delta}_1 - \dot{\Delta}_2) \quad (3.8)$$

$$h_p = -\ln(e) / \sqrt{\pi^2 + (\ln(e))^2} \quad (3.9)$$

Where P = external force when pounding occurs, K_p = stiffness, c_p = damping coefficient, h_p = damping ratio, e = coefficient of restitution.

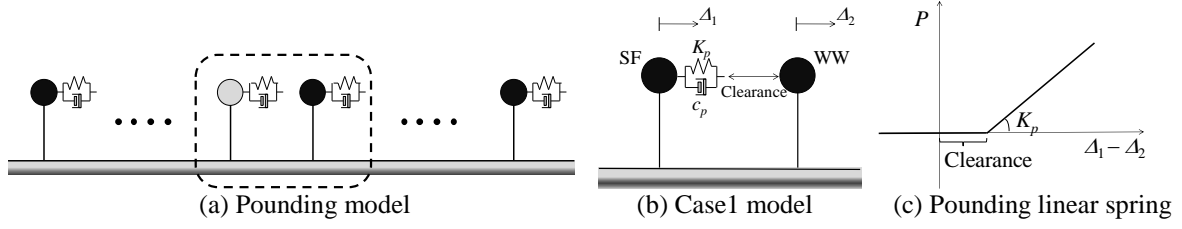


Figure 3.9. Description of pounding model

3.4.2. Result of simulation analysis

Simulation analysis is executed to inspect the pounding model. In this paper, The models are SF and WW of Case 1 and input wave is sinusoidal pulse $T_p = 1.0s$. The parameter of pounding linear spring and dashpot is determined in parameter study in 3.4.3. Newmark β method is used for time historical analysis. The model of analysis is SFOD and the restoring force characteristic is the superposition of Bi-linear, Slip and Linear spring in Fig. 3.10. This restoring force characteristic is easy to make modelling. Slip is tri-linear skeleton curve. Stiffness at the time of unloading is initial stiffness.

First, simulation analysis without pounding is executed in Fig. 3.11 and the parameters are determined to fit the experimental result. Note that areas of skeleton curve of the experiment and simulation analysis are the same. Table 3.2 shows the parameter of skeleton curve of SF and WW (Case 1). Figure 3.12 shows the result of simulation analysis with pounding. Although deformation angle when pounding is a little bit different in force - displacement relation, simulation analysis reproduces the experiment approximately. Figure 3.13 indicates time history of pounding simulation analysis.

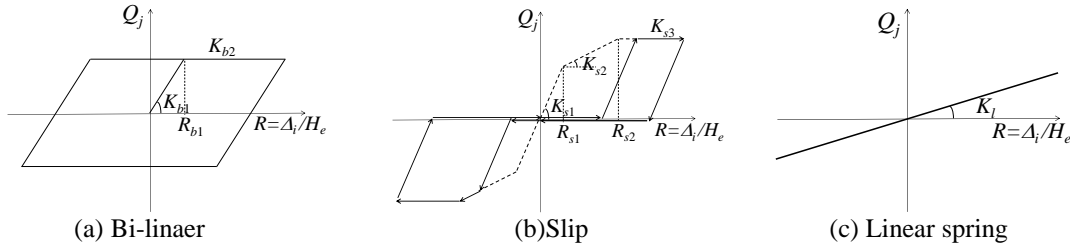


Figure 3.10. Skeleton of SDOF model

Table 3.2. Parameter of skeleton curve

	Mass	Height	Initial Damping ratio	Bi-linear		
				Initial stiffness	Second stiffness	Initial intersection
	M_e (kg)	H_e (mm)	h_0	K_{b1} (kN/mm)	K_{b2} (kN/mm)	R_{b1} (rad)
SF	1124.5	2625	0.03	0.0082	0	0.005
WW	1155.5	2625	0.03	0.0434	0	0.002
	Slip					Linear
	Initial stiffness	Second stiffness	Third stiffness	Initial intersection	Second intersection	Stiffness
	K_{s1} (kN/mm)	K_{s2} (kN/mm)	K_{s3} (kN/mm)	R_{s1} (rad)	R_{s2} (rad)	K_l (kN/mm)
SF	0.012	0.0053	0	0.025	0.050	0.0038
WW	0.130	0.0455	0	0.002	0.007	0.0266

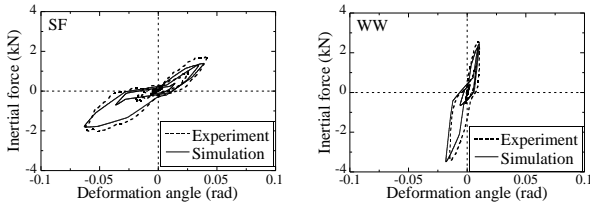


Figure 3.11. Simulation analysis without pounding

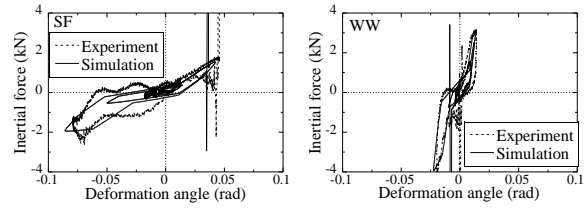
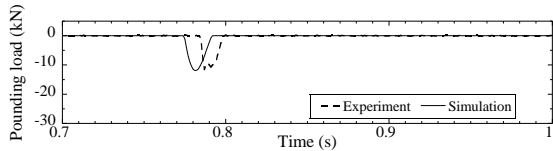
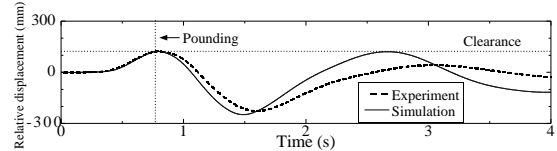


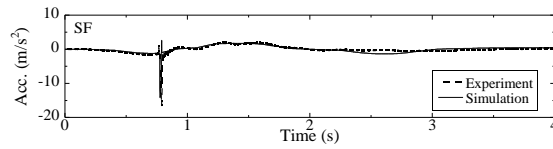
Figure 3.12. Simulation analysis with pounding



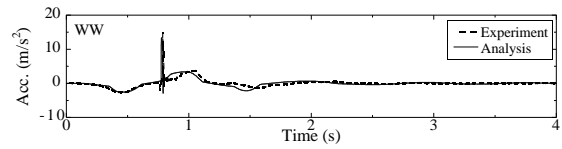
(a) Pounding load



(b) Relative displacement



(c) Acceleration of SF



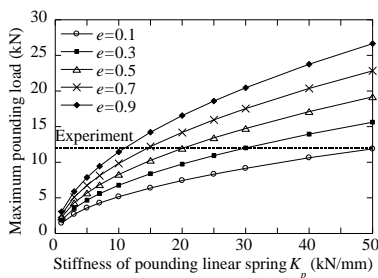
(d) Acceleration of WW

Figure 3.13. Comparison between simulation analysis and the experiment

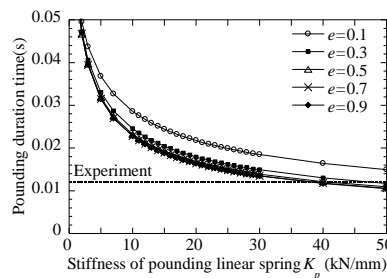
3.4.3. Effect of the parameter of pounding linear spring and coefficient of restitution

Figure 3.14 shows how maximum pounding load, pounding duration time and maximum response displacement after pounding change depending on the parameter pounding linear spring K_p and coefficient of restitution e .

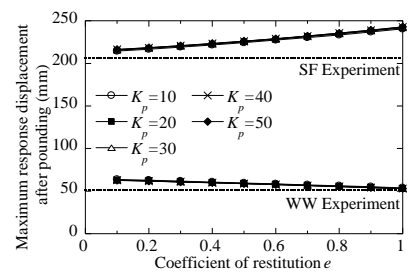
K_p is less related to maximum response displacement after pounding although K_p affects maximum pounding load and pounding duration time. e is less related to pounding duration time although e affects maximum pounding load. Figures 3.14(c) indicates that maximum response displacement after pounding changes only 30mm and the error doesn't affect so much. In conclusion, seismic damage prediction with pounding using maximum response displacement after pounding does not affect the parameter of pounding linear spring or the coefficient of restitution.



(a) Maximum pounding load



(b) Pounding duration time



(c) Maximum response displacement after pounding

Figure 3.14. Parametric study of K_p and e

4. CONCLUSIONS

The objective of this study is to establish a method of evaluating whether a pounding arises or not between adjacent traditional wooden houses especially by pulse-like strong ground motions arisen from inland earthquakes. The major findings obtained from the research are summarized as follows:

- 1) In random vibration, the “spectral difference (SPD) rule” [Kasai et al. (2004)] which evaluates relative displacement based on equivalent period and damping ratio of houses is effective to evaluate the interval between two houses. When shaken by a pulse wave, the evaluation accuracy of relative displacement falls compared with the case of random vibration. Therefore, we present the method to evaluate the interval between two houses from the relation between the period of pulse-like strong ground motions and the natural period of two houses, without using the SPD rule.
- 2) If pounding occurs, their behavior can be simulated by non-linear time history response analysis with a pounding spring between two houses. From parameter study, the stiffness of pounding linear spring and coefficient of restitution do not influence so much to the maximum deformation angle of the buildings.

AKNOWLEDGEMENT

A part of this research was supported by Grants-in-Aid for Scientific Research (A) (No. 22246072) and TOSTEM Foundation for Construction Materials Industry Promotion.

REFERENCES

- Y. Hayashi, S. Higa, Y. Hasebe, T. Morii, M. Matsuda, and M. Koshihara. (2009). Seismic performance evaluation for groups of historic wooden houses, *ICOSSAR'09*. pp.890-896.
- M. Yamada, Y. Suzuki, M. Gotou and H. Shimizu. (2004). Dynamic and static tests of wooden frames for evaluation of seismic performance, *Journal of Structural and Construction Engineering, Architectural Institute of Japan*, **No.582**, pp. 95-102. (in Japanese)
- T. Morii, M. Miyamoto, H. Takahashi, Y. Hayashi. (2010). Influence of $P\Delta$ effects on deformation capacity of wooden frame structure, *Journal of Structural and Construction Engineering, Architectural Institute of Japan*, **No.650**, pages 849-857. (in Japanese)
- Y. Hayashi, A. Nii and T. Morii. (2008). Evaluation of building damage based on equivalent performance response spectra. *The 14th World Conference on Earthquake Engineering*.
- K. Kasai and B. T. Tran. (2004). A Simplified method to predict peak value and trend of seismic relative motion between adjacent buildings. *Journal of Structural and Construction Engineering, Architectural Institute of Japan*. **No.582**, pp.47-55.
- Y. Hayashi. (2002). Evaluation of seismic design load based on equivalent-performance response spectra. *The 11th Japan Earthquake Engineering Symposium*. pp. 651-656. (in Japanese)
- K. Suzuki, H. Kawabe, M. Yamada and Y. Hayashi. (2010). Design response spectra for pulse-like ground motions. *Journal of Structural and Construction Engineering, Architectural Institute of Japan*. **No. 647**, pp. 49-56, (in Japanese)
- A. Shibata. (1981). Analysis of earthquake resistant structure. *Morikita shuppan*. (in Japanese)
- Y. Araki, M. Koshihara, Y. Ohashi and I. Sakamoto. (2004). A study on hysteresis model for earthquake response analysis of timber structures. *Journal of Structural and Construction Engineering, Architectural Institute of Japan*. **No. 579**, pp. 79-85, (in Japanese)